

Supporting Information

Schaller et al. 10.1073/pnas.1107540108

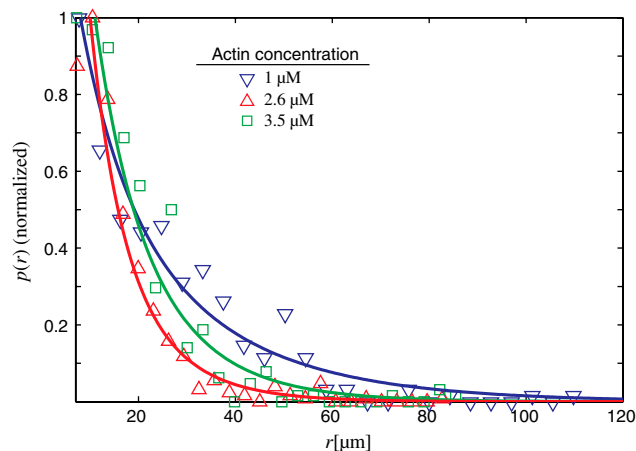


Fig. S1. Decay of the curvature radii as a function of the actin concentration. Independent of the actin concentrations the distributions decay according to $p(r) = a_1 \cdot \exp(-r/l_1) + a_2 \cdot \exp(-r/l_2)$, shown as solid lines. For the lowest actin concentration (1 μM , blue curve) parameters are $a_1 = 0.59\mu\text{m}$; $a_2 = 0.41\mu\text{m}$; $l_1 = 9.34\mu\text{m}$; $l_2 = 24.62\mu\text{m}$. For the intermediate actin concentration (2.6 μM , red curve) $a_1 = 0.53\mu\text{m}$; $a_2 = 0.47\mu\text{m}$; $l_1 = 5.10\mu\text{m}$; $l_2 = 12.57\mu\text{m}$ was found and for the highest actin concentration (3.5 μM , green curve) $a_1 = 0.59\mu\text{m}$; $a_2 = 0.41\mu\text{m}$; $l_1 = 8.29\mu\text{m}$; $l_2 = 15.01\mu\text{m}$ resulted. The motor density was adjusted to $\sigma_m = 90 \text{ nM}$ and the fascin concentration was $c = 0.5 \mu\text{M}$.

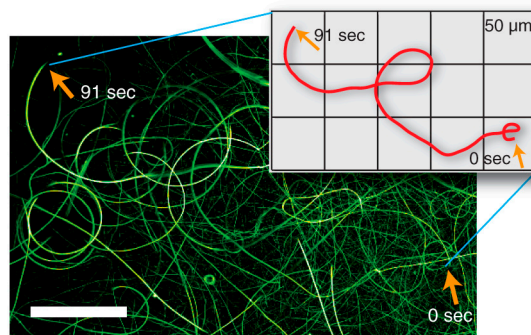


Fig. S2. Time overlay of a moving actin-fascin string. Actin-fascin strings move on circular trajectories. The thicker the strings get, the higher their directional persistence. As a consequence variations of a given curvature happen increasingly less frequent and have less effect. The motor density was adjusted to $\sigma_m = 90 \text{ nM}$, the actin concentration was $\rho = 3 \mu\text{M}$ and the fascin concentration was $c = 0.5 \mu\text{M}$. The scale bar is 50 μm .

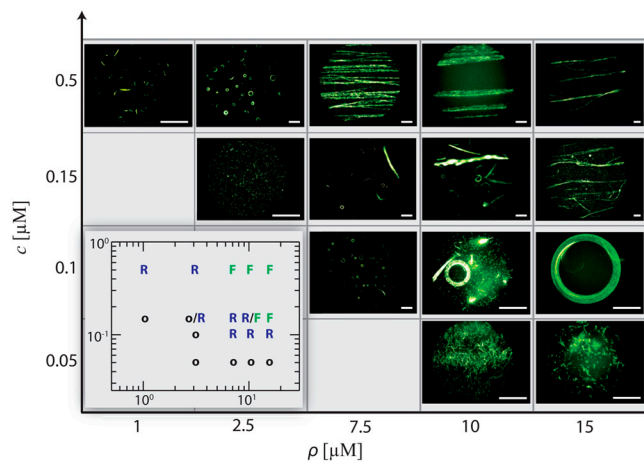


Fig. S3. Phase diagram as a function of the actin ρ and fascin concentration c . For high actin and fascin concentration the systems evolves into a frozen steady state that is characterized by coherently moving streaks or fibers (F). For intermediate concentrations of actin and fascin the frozen active state is given by the ring phase (R). At low fascin concentrations the steady state is characterized by persistent fluctuations on the single filament level and no frozen steady state emerges (o). All scale bars are 50 μm and the motor density was adjusted to 90 nM.

Ring Closure

video 2 - supplement to Fig. 2

parameters: $\rho = 10 \mu\text{M}$,
 $c = 0.1 \mu\text{M}$, $\sigma_m = 90 \text{ nM}$



Movie S2. The emergence of stable curvatures relies on two mechanisms: the ring closure and the freezing of a current curvature (actin concentration $\rho = 3 \mu\text{M}$, motor concentration $\sigma_m = 90 \text{ nM}$, fascin concentration $c = 0.2 \mu\text{M}$, labeling ratio 1:16).

[Movie S2 \(MOV\)](#)

Simulations

video 3 - supplement to Fig. 3

ARNOLD SOMMERFELD
CENTER FOR THEORETICAL PHYSICS

parameters: $\omega = 0.1$, $\lambda = 0.4$, $\alpha = 1.0$, $\Theta_c = 10^\circ$

Movie S3. Emergence of rotating rings in the cellular automaton simulations and coexistence of open and closed rings ($\omega = 0.1$, $\lambda = 0.4$, $\alpha = 1.0$ and $\theta_c = 10^\circ$).

[Movie S3 \(MOV\)](#)

Coherently Moving Streaks

video 4 - supplement to Fig. S3



parameters: $\rho = 10 \mu\text{M}$, $c = 0.5 \mu\text{M}$, $\sigma_m = 90 \text{ nM}$

Movie S4. Above a certain material density curved trajectories are no longer possible and the actin-fascin structures are forced on straight trajectories; extended actin-fascin streaks evolve that successively merge and coarsen, leading to a large scale symmetry breaking (actin concentration $\rho = 10 \mu\text{M}$, motor concentration $\sigma_m = 90 \text{ nM}$, fascin concentration $c = 0.5 \mu\text{M}$, labeling ratio 1:32).

[Movie S4 \(MOV\)](#)